DOI: 10.1070/RCR4681

Modern electron microscopy in the study of chemical systems at the boundary of organic synthesis and catalysis †

Valerii I. Bukhtiyarov,[a, b] Vladimir I. Zaikovskii,[a, b] Alexey S. Kashin,[c] Valentine P. Ananikov [c, d]

[a] *G.K.Boreskov Institute of Catalysis, Siberian Branch of the Russian Academy of Sciences prosp. Akademika Lavrentieva 5, 630090 Novosibirsk, Russian Federation*
[b] *Novosibirsk State University ul. Pirogova 2, 630090 Novosibirsk, Russian Federation*
[c] *N.D.Zelinsky Institute of Organic Chemistry, Russian Academy of Sciences Leninsky prosp. 47, 119991 Moscow, Russian Federation*
[d] *Saint-Petersburg State University Universitetskaya nab. 7 – 9, 199034 St Petersburg, Russian Federation*

Electron microscopy, which has become a routine tool of materials science, heterogeneous catalysis, metallurgy and some other areas, is currently attracting increasing attention of researchers working in the area of fine organic synthesis. The modern capabilities for direct visualization of micro- and nano-objects suitable for characterization of electron beam-sensitive molecular and hybrid organic systems extend the scope of applicability of electron microscopy in chemistry. The review describes representative examples of electron microscopic investigations at the boundary of organic synthesis and catalysis.
The bibliography includes 114 references.

Contents

I. Introduction 1198
II. Electron microscopy in the studies of heterogeneous catalysis and surface processes 1200
III. Electron microscopy in the studies of organic molecular and hybrid systems 1206
IV. Conclusion 1211

I. Introduction

Organic synthesis and catalysis form the basis of modern industry and occupy a top position in high-tech economy sectors.[1, 2] Currently, an interdisciplinary area is being formed at the boundary of these fields, which would largely affect the state of chemical science in the near future.[1 – 3] A key aspect determining the progress in this interdisciplinary field is understanding of chemical phenomena and investigation of chemical reaction mechanisms. The complexity of synthesized molecular systems is so high that the search for new reactions and development of new catalysts by screening of options and traditional successive optimization are either no longer possible or cost-prohibitive. The prob-

† Dedicated to Academician O.M. Nefedov on the occasion of his 85th birthday.

V.I.Bukhtiyarov. Academician, Doctor of Chemical Sciences, Professor, Director of the BIC SB RAS, Head of the Chair at the NSU.
Telephone: +7(383)330 – 6771, e-mail: vib@catalysis.ru
Current research interests: heterogeneous catalysis, surface science, physical methods of surface investigation, catalytically active functional nanomaterials.
V.I.Zaikovskii. Candidate of Chemical Sciences, Senior Researcher at the BIC SB RAS, Associate Professor at the NSU.
Telephone: +7(383)326 – 9762, e-mail: viz@catalysis.ru
Current research interests: heterogeneous catalysis, surface science, electron microscopy.
A.S.Kashin. Candidate of Chemical Sciences, Researcher at the ZIOC RAS.
Telephone: +7(499)135 – 9094, e-mail: a.kashin@ioc.ac.ru
Current research interests: catalysis, organic synthesis, electron microscopy, X-ray spectroscopy
V.P.Ananikov. Corresponding Member of the RAS, Doctor of Chemical Sciences, Professor, Head of the Laboratory of Metal Complex and Nanoscale Catalysts at the ZIOC RAS, Head of a Laboratory of the SPbU.
Telephone: +7(499)135 – 9094, e-mail: val@ioc.ac.ru
Current research interests: catalysis, organic synthesis, nanotechnologies, graphene chemistry, photochemistry, molecular modelling, physical chemistry.

Received 8 July 2016
Translation: Z.P.Svitanko

© 2016 Russian Academy of Sciences and Turpion Ltd.

lem of constructing 'molecular complexity' with the previously inaccessible atomic precision appeared in response to the need for selective organic reactions for the preparation of complex molecules.[3,4]

The application of physicochemical methods in the research into the nature of chemical reactions in the listed fields has its specific character. The reactions related to fine organic synthesis most often proceed in solutions and homogeneous catalyst systems where nuclear magnetic resonance spectroscopy and mass spectrometry are the key methods.[5–7] The use of electron microscopy in this field was quite rare until recently.

In the studies of heterogeneous catalysis and surface phenomena, electron microscopy is the main method with a many-year application experience, providing unique information on the micro- and nanostructure of heterogeneous catalysts. This is caused by high spatial resolution of, first of all, transmission electron microscopy, which provides effective retrieval of structural parameters such as the shape and size distribution of deposited oxide and metal particles and, in the high-resolution mode, also interlayer spacings, interatomic distances, the structure of boundaries between particles of different composition, *etc*.

The transmission electron microscope with accelerating voltage of 1 MV and a coherent electron beam operating on a cold field emission source designed by Hitachi (Japan) in 2000 was the pioneering microscope with a resolving power better than 0.5 Å.[8] More recently, the successful operation of a Hitachi H-3000 transmission electron microscope with accelerating voltage of up to 3.5 MV was demonstrated; this instrument was suitable for examination of thick samples and gave 3D images of items with a thickness of > 300 nm.[9]

It is worth mentioning that high-resolution transmission electron microscopy has long been not only a method for obtaining mechanistic parameters or morphological characterization of samples. This is due, first of all, to attainment of a spatial resolution of < 1 Å for microscopes manufactured by top companies such as FEI (USA), JEOL (Japan), Hitachi and so on. The progress in this field was enabled by the design of spherical aberration correctors for electromagnetic lenses (Cs-correctors), which minimize the image distortion.[10,11] Aberration-free lenses are used to produce a narrow electron probe in scanning transmission electron microscopy and high-resolution electron microscopy. The former technique generates large arrays of analytical digital information in pixel picture elements. As a consequence, the obtained images are suitable for observing single atoms of the crystal lattice;[12–15] simultaneously, it is possible to perform elemental and chemical analyses by energy dispersive X-ray spectroscopy and electron energy loss spectroscopy at the atomic level of resolution.[14,16]

Currently, SU9000 (Hitachi), ARM-200, 300 (JEOL) and TITAN (FEI) instruments provide the highest spatial resolution down to 0.4 Å. This allows visualization of separate heavy atoms (Pd, Au, Pt and so on) in standard modes. Moreover, intensity analysis of images of single atoms or small clusters leads to conclusions about the nature of a metal (the greater the metal atomic mass, the higher the intensity), which is very important for studying supported bimetallic catalysts.

One more recent achievement of electron microscopy is the possibility of direct observation of sample evolution during a chemical reaction conducted *in situ*. By *in situ* studies with digital recording of the state of the sample on a real time basis, researchers obtain qualitatively new data on the transformations of a catalyst during the operation. The most advanced electron microscopes are suitable for investigations in a controlled gas phase at pressures up to 0.1 atm and temperatures up to 1000 °C. Finally, high-angle annular dark field scanning transmission microscopy can accomplish 3D tomography of samples.[17] The listed capabilities of modern microscopes are optional and also serve as a prerequisite for electron-microscopic examination at a still higher level. However, it is noteworthy that, despite the advances made in the development of new procedures of electron-microscopic imaging, there are typical problems, which must be taken into account; otherwise, the achievements mentioned above would come to nothing, even in the study of standard heterogeneous catalyst systems, not to mention microscopic investigations of organic reactions.

As representative examples of the development of modern electron microscopy and its demanded applications, it is pertinent to consider determination of 3D structures of nanocrystals,[18,19] study of biological and pharmaceutical systems[20,21] and study of multicomponent catalyst systems.[22–25] Microscopic investigations directly in the liquid phase are of principal significance for fine organic synthesis and catalysis.[26–30]

An interesting current trend is transfer of knowledge and research experience gained by electron microscopy from heterogeneous catalysis and surface science to the field of organic synthesis. In this case, microstructural studies serve as an important linking unit, which makes this field interdisciplinary. The present review considers the key methodical aspects and particular examples of practical use of electron microscopy in these boundary areas.

The progress in the electron microscopy itself (both the methodological development and advancement of equipment) is caused, to a large extent, by the need to study catalysts and surface phenomena. These applications of electron microscopy are considered in Section II of the review.

Organic molecular and hybrid systems have long remained a 'sticking point' for high-resolution electron microscopy because of the sensitivity of samples, which can be readily destroyed by an electron beam. It was only recently that the development of microscopic technical equipment and appearance of new-generation field emission devices brought investigation of organic systems to an operating level. In this review, this application of electron microscopy is considered in Section III.

Examples of practical applications of electron microscopy presented in the review were taken from publications of the last five years and from experimental works performed with participation of the authors (for instance, photomicrographs shown in Figs 1, 4, 7 and 11 had not been included in the relevant original publications because of size limitation).

The following abbreviations are used in the review:

BF — Bright Field;

BF-STEM — Bright Field Scanning Transmission Electron Microscopy;

BMIM — 1-Butyl-3-Methylimidazolium;

DF — Dark Field;

EDX (EDX Spectroscopy) — Energy Dispersive X-Ray Spectroscopy;

EDS — Energy Dispersive X-Ray Spectroscopy (same as EDX);

EELS — Electron Energy Loss Spectroscopy;
EXAFS (EXAFS Spectroscopy) — Extended X-Ray Absorption Fine Structure Spectroscopy;
FFT — Fast Fourier Transform;
FIB — Focused Ion Beam;
HAADF-STEM — High Angle Annular Dark Field Scanning Transmission Electron Microscopy;
HRTEM — High-Resolution Transmission Electron Microscopy;
MOF— Metal-Organic Framework;
MWCNT — Multi-Walled Carbon Nanotubes;
NFs — Nanofibers;
Ox — Oxidative Conditions;
SAED — Selected Area Electron Diffraction;
SEM — Scanning Electron Microscopy;
STEM — Scanning Transmission Electron Microscopy;
TEM — Transmission Electron Microscopy;
XRD — X-Ray Diffraction;
XPS — X-Ray Photoelectron Spectroscopy.

II. Electron microscopy in the studies of heterogeneous catalysis and surface processes

II.1. Methodological details of electron-microscopy experiments

Most often, heterogeneous catalysts are nanopowders possessing the desired texture and porosity and formed as pellets. In supported catalyst systems, the active component is deposited on various porous supports, which are not always inert and can also exhibit catalytic properties (simple and complex oxides, zeolites, carbon and so on). In addition, there is a large class of block systems in which the catalyst is supported on the walls of cellular blocks as a secondary layer; these systems possess high thermal and mechanical stability. The most extensive class of such systems is represented by automotive catalysts for exhaust gas purification. In the case of electrochemical reactions, the catalyst is deposited on the ends of electrically conducting carbon rods. Despite different sample shapes and deposition sites of the active component, a TEM examination requires pretreatment of all samples according to one of standard procedures.

It is worth noting, first of all, that image formation mechanisms and sample preparation procedures are different for scanning and transmission electron microscopy. The accelerating voltages in SEM are of the order of several tens kiloelectron-volt (most often, not more than 40 keV). The SEM images are formed upon analysis of the intensities of secondary or reflected (more sensitive to the surface topography) electrons. The objective of SEM is to study the surface topology at both high and low magnifications. In order to enhance the spatial resolution, one can decrease the accelerating voltage down to several hundred volts. Investigation of dielectrics requires sputtering of heavy metals (Au, Pt, Ir and so on) as layers, desirably as thin as possible. In the case where, apart from imaging, it is necessary to determine the elemental composition by EDX, conductive carbon layers have to be used, thus sacrificing spatial resolution. It should be mentioned that obtaining SEM images at atomic resolution is often inexpedient. Atomic resolution surface examination is carried out by means of probe or atomic force microscopy.

Sample preparation for a TEM examination includes a decrease in the sample thickness to make it transparent for fast electrons at an accelerating voltage of 100 – 400 keV or sample dispersion into particles several tens of nanometres large. The technique of focused ion beam thinning (most often, using gallium ions at an accelerating voltage of 30 kV) serves for sample preparation from single-crystalline layers, semiconductor heterostructures and other items that are of prime importance in microelectronics. Benchmark companies manufacture unique high-tech devices for sample preparation, *e.g.*, such as FIB (GATAN, USA).

However, studies of heterogeneous catalysts as nanosized powders do not require this type of equipment. The most popular method of catalyst preparation for TEM investigation is the classical powder dispersion method and, first of all, its type called the method of liquid suspensions. This sample preparation procedure is used very often and will not be additionally described here. We would only like to mention that the use of 10 – 20 nm-thick perforated carbon films is important as they retain the dispersed particles and hence the interfering influence of the amorphous carbon substrate can be avoided.

Biological products are most often prepared for investigation by ultramicrotomy, which means cutting the specimens into extremely thin sections by diamond or glass knives. The samples are stabilized in a polymeric embedding medium. Limitations of this method are associated with instability of the embedding medium (epoxy resin) on exposure to an electron beam under vacuum; this hinders sample examination at high magnifications.

It is also noteworthy that for addressing unusual problems that can be solved by electron microscopy (electron tomography, TEM examination *in situ* in a controlled gas environment and so on), a tailored design for sample chambers and holders of the electron microscope is required.

II.2. Application of electron microscopy for solving particular research problems

The active component of a heterogeneous catalyst is usually represented by nano-sized particles or aggregates of such particles, in some cases, with a complex composition and structure. Targeted synthesis of active catalysts stable throughout chemical processes requires detailed investigation of the particle properties by means of the most informative physicochemical methods.

Electron microscopy is the only method suitable for observing the atomic structure of a multicomponent catalyst with a high spatial resolution. The use of conventional and scanning transmission modes in modern electron microscopes and combining the imaging mode with X-ray spectroscopy and electron energy loss spectroscopy serve for analytical investigations with determination of the elemental composition of local sites down to sizes of single atoms. Furthermore, EELS can be used to analyze chemical bonds formed by atoms in catalyst particles.

In what follows we will consider some aspects of electron-microscopy examination of catalyst nanoparticles and its role for investigation of organic reaction systems.

II.2.a. Supported metal catalysts

Most of supported metal catalysts are rather stable on exposure to electron beam; therefore, they can be studied by electron microscopy. In most cases, they contain a metal with a high mass density (Pt, Pd, Ru, Au, Ag, Ni, Co, *etc.*) deposited on a porous material. The supports are usually

represented by oxides (Al_2O_3, SiO_2, TiO_2, MgO, *etc.*) or carbon materials of various structures with a moderate density. It is also necessary to take into account the possibility of metal oxidation during the sample preparation. Platinum and gold cannot be oxidized, Pd, Ru and Ag are slightly oxidizable, while metals like Fe, Ni and Co are oxidized rather rapidly.

The images obtained by microscopy are two-dimensional and reflect the structure of three-dimensional catalyst aggregates distributed in space; this is reflected in the image formation details. For imaging, one should take into account both the properties of the catalyst (textural features, chemical composition of particles, radiation and thermal stability of the support and the metal, *etc.*) and the instrumental conditions (electron beam density and focusing, lens aberration and other factors).

Using electron microscopy, it is possible to perform statistical analysis of particle size and to determine parameters such as the statistical average size, standard deviation and so on. Moreover, electron microscopy provides information on the active site location on the surface and in the bulk, texture of the support and the nature of interaction between the metal and the support. Limitations arise in the case of broad multimodal particle size distributions comprising both atomically dispersed particles and particles beyond the nanoscale sizes (>100 nm). The issues of correct imaging of small particles are solved using mathematical modelling of electron-microscopic images. Below we note some features of application of new electron-microscopy methods for the investigation of supported catalysts.

II.2.b. Examination of supported metal particles and determination of particle size

Z-Contrast method in HAADF-STEM. The best electron-microscopy method for determination of heavy metal particle size on low-density supports is *Z*-contrast (atomic number-based contrast)[10,12,13] implemented in the scanning mode of electron microscopy with inelastic high-angle ($\sim 10^\circ$) electron scattering (HAADF-STEM method). Owing to the quadratic intensity dependence, the HAADF-STEM image of a *Z*-metal particle has high contrast against a lighter support background. With instruments of spatial resolution of ~ 1 Å equipped with dark field detectors, it is possible to see single atoms in the images. The atomic structure charge density is directly projected on the plane of the HAADF-STEM image in which the positions of single atoms can be discerned. Thus, the achievable limit of detection of heavy atoms is the single atom size; the HAADF-STEM determinations of particle sizes are highly reliable.

Detailed investigations at the atomic level enable determination of the chemical composition and visualization of the crystal lattice geometry for the sample. There are quite a few examples of recording clear images with high magnification ($\times 5-10$ million) with atomic structure *Z*-contrast for palladium, platinum, gold and other heavy metal particles. Figure 1 presents the HAADF-STEM images of Au particles incorporated in the cavities of a macrocyclic cavitand, cucurbit[6,7]uril. This organic compound is able to incorporate host molecules and bind them in the cavities.[32] It can be seen that gold occurs in the cavities in the form of atoms or clusters of $\leqslant 1$ nm size. The data on the size of the smallest metal particles are consistent with the results of EXAFS studies using synchrotron radiation.[31] Meanwhile, gold located on the outer surface of the cavitand forms coarsely dispersed particles of 5 – 20 nm size.

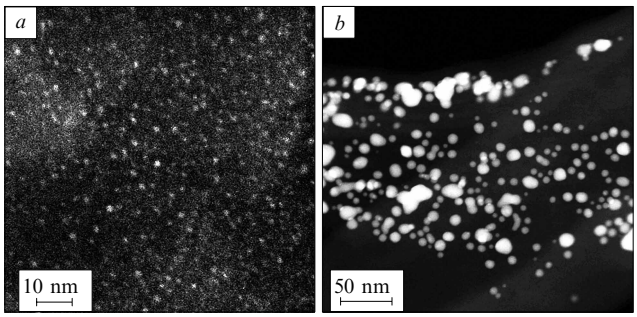


Figure 1. HAADF-STEM images of Au particles embedded in the organic cavitand cucurbit[6,7]uril. The micrographs were made by V.I.Zaikovskii (BIC SB RAS) by a procedure reported in Ref. 31. (*a*) Particles of <1 nm size located in inner molecular cavities of the cavitand; (*b*) particles of 5 – 20 nm size located on the outer surface of large aggregates.

Other examples of reaching a subnanometre and even atomic resolution in the studies of supported metal catalysts are shown in Figs 2 and 3. Indeed, the spatial distribution of up to 0.5 nm nanoparticles of the PdCu alloys attached to the surface of porous γ-Al_2O_3 can be clearly seen in the HAADF image of the commercial PdCu/γ-Al_2O_3 catalyst (Fig. 2 *a*).[11]

The high-resolution HAADF images of the precursor of the Au/TiO_2 catalyst for low-temperature CO oxidation (see

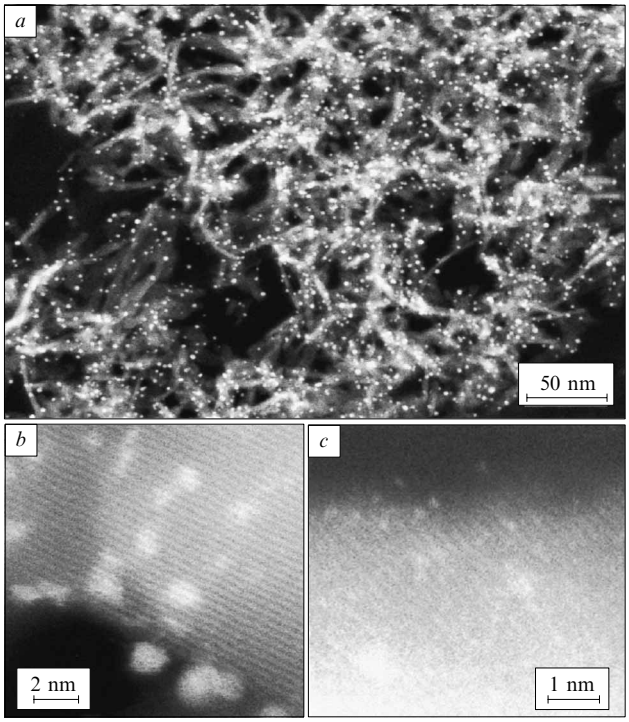


Figure 2. HAADF images of the PdCu/γ-Al_2O_3 alloy (*a*), precursor of the 5 mass % Au/TiO_2 catalyst with Au clusters and nanoparticles (*b*) and single Au atoms (*c*) attached to the titanium dioxide surface.[11]

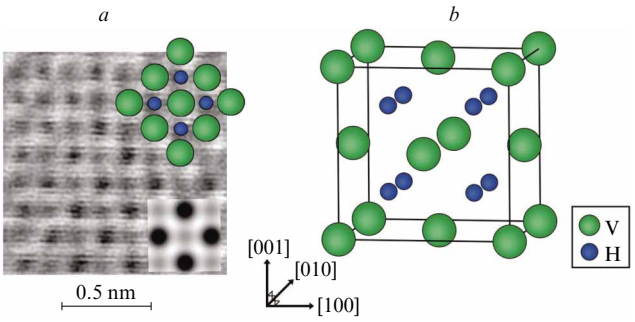


Figure 3. BF-STEM image of the hydride VH_2 obtained on a JEM-2100F electron microscope.[14]
The hydrogen atoms are located in space between the vanadium crystal lattice points. (*a*) BF-STEM image of a vanadium hydride (VH_2). The overlay shows the lattice projection, the underlay is the simulated image (for 5 nm thick sample); (*b*) model of the VH_2 structure.

Fig. 2 *b*,*c*) show gold particles, clusters and single atoms attached to the titanium dioxide surface. In the images, it is also possible to trace the interaction of Au nanoparticles with TiO_2 surface defects. Presumably, the oxygen vacancies on the titanium dioxide surface serve as the sites for attachment of molecules of the active component precursor and as nucleation centres for gold nanoparticles during the subsequent reductive treatment.

As the most recent advance in the atomic imaging, consider the publication[14] in which the STEM images of hydrogen atoms in the hydride VH_2 structure (see Fig. 3) were obtained using a specially re-designed JEM-2100F electron microscope equipped with a spherical aberration corrector; the resolution was 0.1 Å.

A study of the properties of mono- and bimetallic catalysts supported on materials prepared from layered aluminium magnesium hydroxides showed them to be efficient in the dehydrogenation of hydrocarbons.[33, 34] The structure of the hydroxide precursor affects the attachment of metal complexes and their location in the layered material. The TEM images of samples obtained by exchange of interlayer anions in hydrotalcite (Mg : Al = 3.3) with $[PtCl_6]^{2-}$ are shown in Fig. 4 *a*,*b*. The *Z*-contrast in the HAADF-STEM image of a 1 mass % $Pt/MgAlO_x$ sample reduced at 450 °C shows only minor signs of regular atomic structure of polyatomic platinum clusters of 1 – 3 nm size located in the porous $MgAlO_x$ structure (see Fig. 4 *b*). If the platinum content is increased to 10 mass %, there are two-dimensional regular structures with a thickness close to the interlayer spacing (d_{003} = 0.75 nm) of the initial aluminium magnesium hydroxide, apart from the platinum clusters (see Fig. 4 *c*).[33] The partial replacement of Mg^{2+} cations of the support by Zn^{2+} cations induces, according to XPS data, $Pt^{\delta-} - Zn^{\delta+}$ interaction, which has a dispersing effect on the catalyst active component and increases the catalyst stability during propane dehydrogenation to propene.[34]

However, it is fairly difficult to determine the positions of light atoms in a material structure using commercial electron microscopes;[35, 36] to this end, additional procedures are needed. A combination of EELS and HAADF-STEM techniques was used to detect nitrogen atoms[34] on carbon in nano-sized palladium catalysts for CO oxidation[36] supported on nitrogen-modified carbon nanofibres (N – CNFs). The HRTEM images demonstrated that the structure of these fibres does not differ fundamentally from the graphite structure. After the reaction, the catalysts were found to contain Pd and PdO particles either located on the surface or partly encapsulated into the near-surface layer of N – CNFs fibres with a graphite-like structure (Fig. 5). This is due to the fact that the doped carbon fibres retain the multilayer graphene structure, but nitrogen atoms replace some of the carbon atoms in the graphene sheet (pyrrole-, pyridine- or graphite-like N-containing rings are formed).[37, 38]

Theoretical considerations indicate that the replacement of carbon by nitrogen may increase the bonding energy between the metal and the modified support by an order of magnitude.[39] Analysis of the reported[35] HAADF-STEM images and EELS spectra of Pd/N – CNFs – Ox catalysts demonstrated a close correlation between Pd and N with Pd nanoparticles being attached to the nitrogen-containing

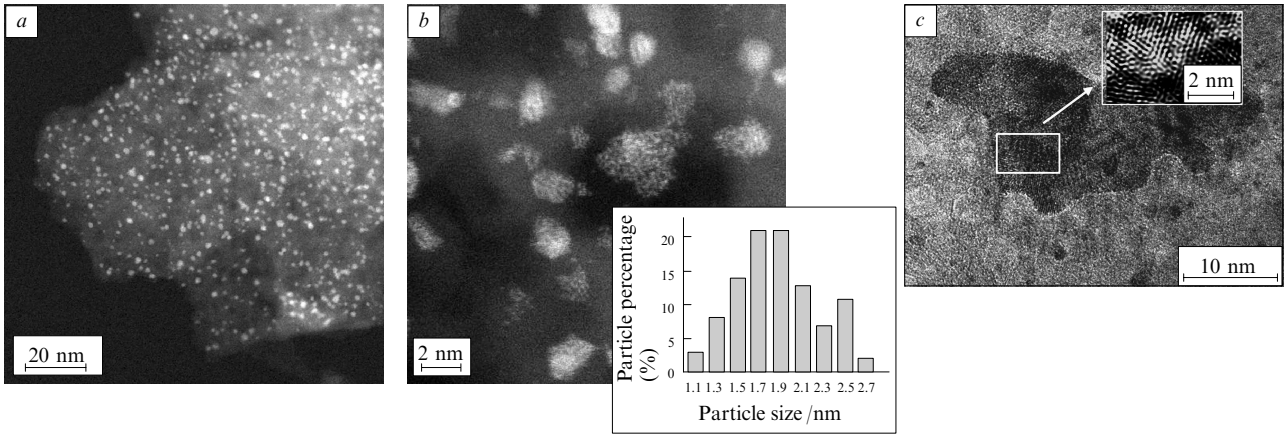


Figure 4. Results of electron-microscopy examination of $Pt/MgAlO_x$ samples of various compositions reduced at 450 °C for 2 h. The micrographs were made by V.I.Zaikovskii (BIC SB RAS) by a procedure reported in Ref. 33.
(*a*, *b*) HAADF-STEM images of medium-size (1.9 nm) Pt clusters; metal content 1 mass %; (*c*) HRTEM image of Pt clusters and isometric and planar particles intercalated into the support; metal content 10 mass %; the inset shows the twin boundary in the Pt structure along the (111) plane after FFT filtration.

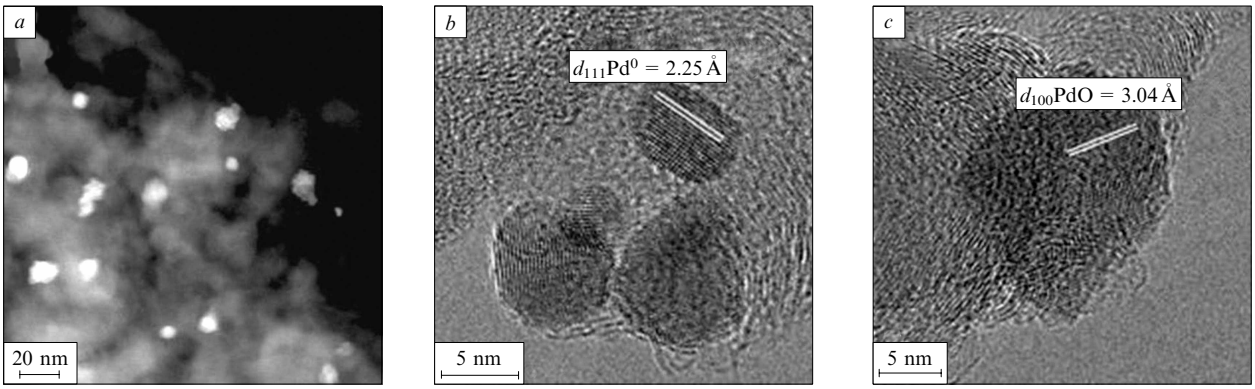


Figure 5. HAADF-STEM image of the Pd/N – CNFs – Ox catalyst (*a*), HRTEM images of Pd^0 (*b*) and PdO (*c*) particles partly encapsulated in the N – CNFs layer. [35]

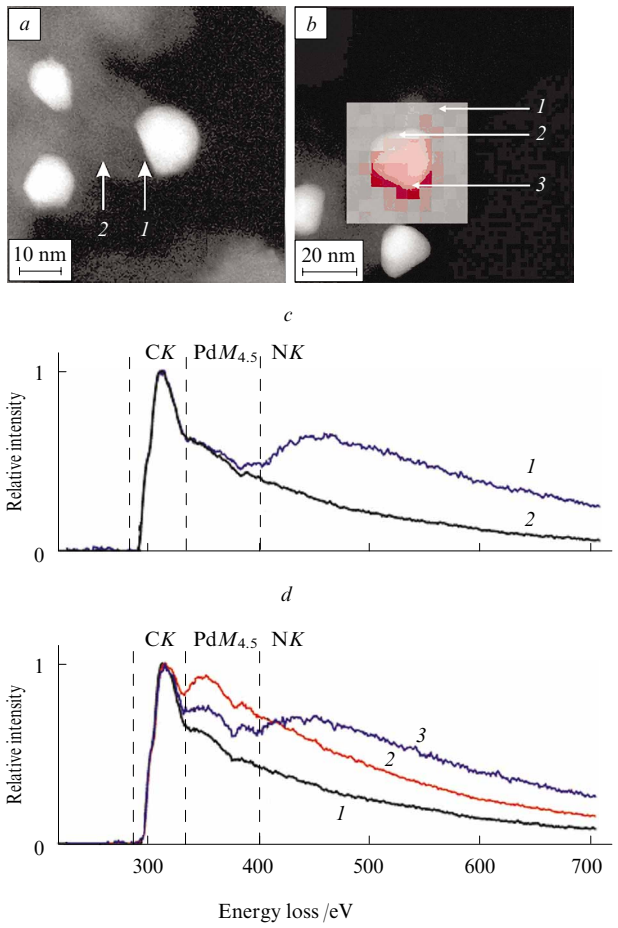


Figure 6. Results of investigation of the Pd/N – CNFs – Ox catalyst.[35]
(*a*) HAADF-STEM image of Pd^0 nanoparticles with a planar interface with the N – CNFs support; (*b*) EELS distribution map of the nitrogen *K*-line, E = 401 eV (red areas) combined with the HAADF-STEM image; (*c*) EELS spectra of the regions marked in Fig. *a*: (*1*) Pd/N – CNFs interface, (*2*) N – CNFs; (*d*) EELS spectra of the regions marked in Fig. *b*: (*1*) N – CNFs, (*2*) Pd^0 nanoparticles, (*3*) Pd/N – CNFs interface.

sites of CNFs (Fig. 6). The oxidation of CO catalyzed by Pd/N – CNFs – Ox was shown to be a self-oscillating reaction over the whole temperature range, while in the same reaction catalyzed by Pd/CNFs, self-oscillations occur only upon cooling of the reactor. The authors assumed that this is caused by a more dispersed state of the active component and strong interaction with the N – CNFs nanofibres, the rate oscillations being due to Pd – PdO redox transitions in the samples involving palladium metal and oxide structures.

Diffraction and phase contrast in TEM imaging. Despite the relative simplicity of using diffraction contrast in the TEM investigations of catalysts, interpretation of images of metal particles deposited on a polycrystalline support with a high specific surface area (Al_2O_3, TiO_2, MgO and so on) is complicated in some cases. The contrast of the images of metal and support crystallites depends on the angle under which they are penetrated by electron beam and varies over broad ranges, which often precludes recognition of particles on the basis of the mass density difference. If the metal and support crystallites have similar morphology and size, as, for example ~5 nm palladium nanoparticles supported on alumina, it is difficult to distinguish between them in the TEM image.

The phase contrast in the HRTEM images allows one to observe the smallest metal particles (Pt, Pd, Ru, Au, *etc.*). Metal particles of sizes below 1 nm provide a high contrast if they are supported on amorphous SiO_2, plate-shaped alumina crystallites or carbon materials. When electron microscopes with a ~1 Å resolution are used, a periodic contrast from the crystal lattice with known parameters is observed in the images, which provides for the most accurate approach to size determination for these particles.

However, the phase-contrast HRTEM images of 1 – 2 nm heavy metal particles are strongly influenced by the Scherzer phase contrast transfer function, which in turn depends on a group of parameters such as electron beam defocusing, the vertical coordinate of the particle position in the aggregate, the objective lens aperture, *etc*. This changes the form of the contrast transfer function for spatially distributed metal particles as well as particle sizes in the HRTEM image. The accurate Scherzer focus is the optimal way of focusing ensuring most adequate determination of sizes of small metal particles (1 – 2 nm).[40]

Thus, the determination of particle distribution for particle size of down to 1 nm requires that the particles be

located in one plane normal to the electron beam. In the case of particles distributed in space, it is necessary to choose narrow defocusing intervals for which the error of measurement of the particle size distribution is minimized. The errors of measurement can be estimated by theoretical calculation of the phase contrast in electron-microscopic images. According to such calculations for heavy metal particles, the particle size can be determined more reliably for > 2 nm sizes.

Structure of the support surface. Epitaxy of supported metal particles. As a rule, crystal lattice planes are resolved more easily in HRTEM images than in STEM images; the latter require more thorough and long-term tuning of the optical system for the formation of a thin electron beam probe. Considering this as well as the mentioned details of phase contrast formation, HRTEM is more efficient for the studies of crystallographic features of real nanosystems and catalysts.

An HRTEM image of the 0.5% Pt/Al_2O_3 catalyst used for complete oxidation of hydrocarbons is shown in Fig. 7 *a*; the spatial position of the sample allows correct calculation of the platinum particle size. It is noteworthy that all metal particles are faceted and oriented in the same way under the influence of epitaxy on the substrate (γ-Al_2O_3) crystal lattice. After statistical treatment of a sufficient number of analogous micrographs, it is possible to construct a relatively accurate size distribution for highly dispersed platinum particles (see Fig. 7 *b*). This enabled accurate determination of average sizes of Pt particles for a series of supported platinum catalysts (from 1 to 10 nm) and to elucidate the correlation between the platinum particle size and activity towards complete methane oxidation.[41]

By means of HRTEM, it was found that the surface structure of crystalline substrate particles is, most often, non-uniform and contains many surface defects. These defects serve as the points of formation of active sites: metal atoms are attached to them during thermal activation of the catalyst to form clusters and nanoparticles.

The support surface relief and crystallographic properties appreciably affect crystallization of metal particles on this surface (despite the polycrystalline state and large specific surface area). Analysis of diffraction-contrast HRTEM images of supported highly dispersed catalysts demonstrated that the epitaxy of particles deposited on a support is an important factor for their stabilization during functioning under fairly drastic conditions.

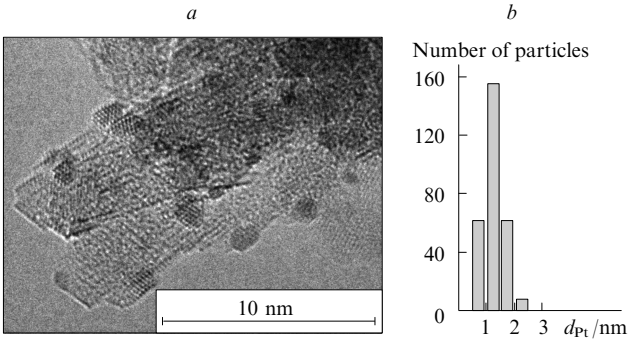


Figure 7. HRTEM image of the 0.5% Pt/Al_2O_3 catalyst (*a*) and Pt particle size distribution (*b*). The micrographs were made by V.I.Zaikovskii (BIC SB RAS) by a procedure reported in Ref. 41.

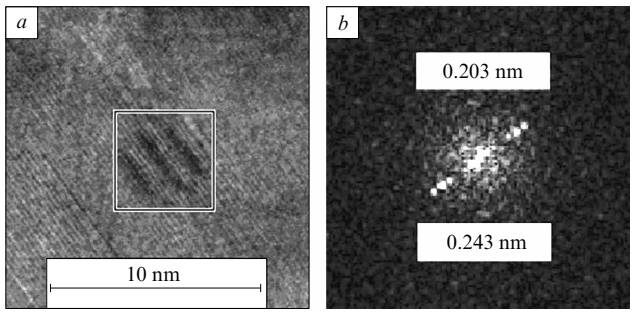


Figure 8. TEM image of the Ni/MgO catalyst.[43]
(*a*) Moire bands from the superimposed Ni and MgO lattices with parallel [111] directions; (*b*) linear arrangement of point reflections on the simulated diffraction pattern with indicated d_{111} interplanar spacings for Ni (above) and MgO (below).

As an example, we will consider a study of the causes of high stability of nickel catalysts supported on porous nickel with a magnesium oxide underlayer.[42,43] A TEM study demonstrated that a large portion of supported nickel crystallites in the catalysts have sizes of 3 – 7 nm and are epitaxially bound to magnesium oxide. After testing for 100 h in methane partial oxidation and steam reforming, the highly dispersed state of nickel metal is retained owing

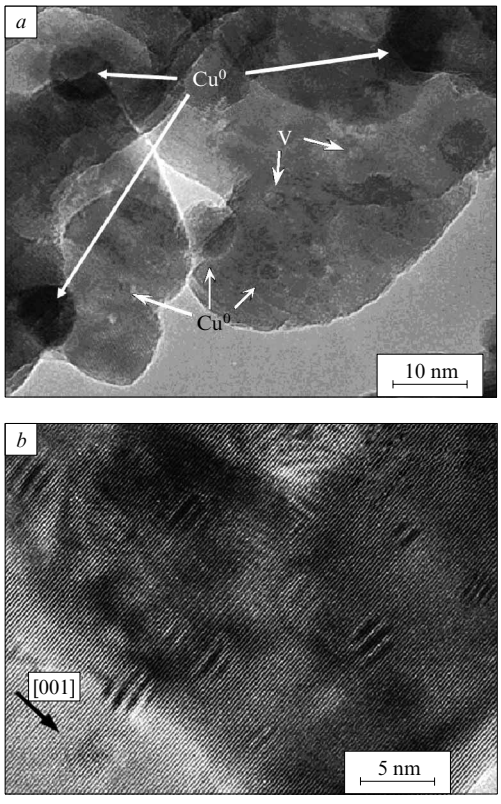


Figure 9. TEM images of the $Cu_{0.08}Zn_{0.92}O$ catalyst after reduction in H_2 at 473 K.[44]
Nanoparticles of Cu^0 (5 – 10 nm) on the surface (*a*) and epitaxial clusters of Cu^0 (2 – 4 nm) in ZnO mesopores (*b*).

to strong epitaxial binding to the MgO underlayer. Furthermore, nickel epitaxy on MgO prevents it from oxidation and the active metal is retained in the dispersed state. The TEM image illustrating the epitaxial deposition of nickel on MgO is shown in Fig. 8 *a*. Electron diffraction modelling (see Fig. 8 *b*) confirmed the complete coincidence of the crystallographic directions, despite some discrepancy in the lattice parameters.

The formation of epitaxial copper clusters was detected in the copper-zinc catalyst $Cu_{0.08}Zn_{0.92}O$ used for the synthesis of alcohols after reduction in H_2 at 473 K (Fig. 9). The epitaxy relationship corresponded to the crystallographic relation: $[\bar{1}\bar{1}2]ZnO||[110]Cu$; $[0001]ZnO||[111]Cu$. The crystallographic regularities of formation of copper metal particles with epitaxy on ZnO was used to determine the mechanism of action and reversible redox regeneration of the catalyst.[44,45]

II.2.c. Other examples

Organic-inorganic hybrid materials based on molybdenum disulfide and polymers are of considerable interest as antifriction coatings, ion conductors, solid electrolytes for batteries and components of photovoltaic cells and light emitting diodes. The possibility of fabricating heterolayer structures, ordered in the nano-sized range, from MoS_2 and polymer monolayers comes from the two-dimensional nature of the molybdenum disulfide crystal structure, which is formed by three-atom-thick S – Mo – S layers connected by van der Waals forces. The hybrid structures were fabricated[46–48] using activated MoS_2 obtained by exfoliation of the material to form monolayers in a liquid medium. It was shown that the chemical nature of the polymers of various types, including polycationic (polydiallyldimethylammonium chloride, polyhexamethyleneguanidinium chloride and so on) and neutral ones (polyvinylcarbazole, polyethylene oxide, polyvinyl alcohol and so on), affects the structure and ordering of hybrid compounds.

It follows from the XRD, HRTEM and SAED data that, depending on the reaction conditions, the period and the pattern of alternation of heterolayers in the hybrid compounds vary depending on the layer thickness of the polymer guest and packing of its molecules between the MoS_2 layers. The superstructural ordering resulting from charge transfer upon hybrid formation is observed in the MoS_2 atomic structure.

Data of a TEM investigation of the intercalation compound $[C_{18}H_{37}(CH_3)_3N]_{0.35}MoS_2$ containing alkylammonium molecules in the spacings between MoS_2 layers are presented in Fig. 10. The period *C* for the structure in which alkylammonium molecules are perpendicular to the MoS_2 layers is 3.5 nm. However, profile analysis of the image intensity demonstrated that the real structure deviates from this model.

The morphology and structure of MOF samples as Ti – MIL-125, which were used in the liquid-phase catalysis of 2,3,6-trimethylphenol oxidation with hydrogen peroxide to 2,3,5-trimethyl-1,4-benzoquinone, were investigated using a combined HAADF-STEM – EDX, SAED and HRTEM procedure.[49] The catalyst particle size was found to remain invariable throughout at least three operating cycles (Fig. 11). The initially microporous Ti – MIL-125 sample was converted to the mesoporous state after the reaction; this is consistent with low-temperature nitrogen adsorption data. After the first cycle, the sample material

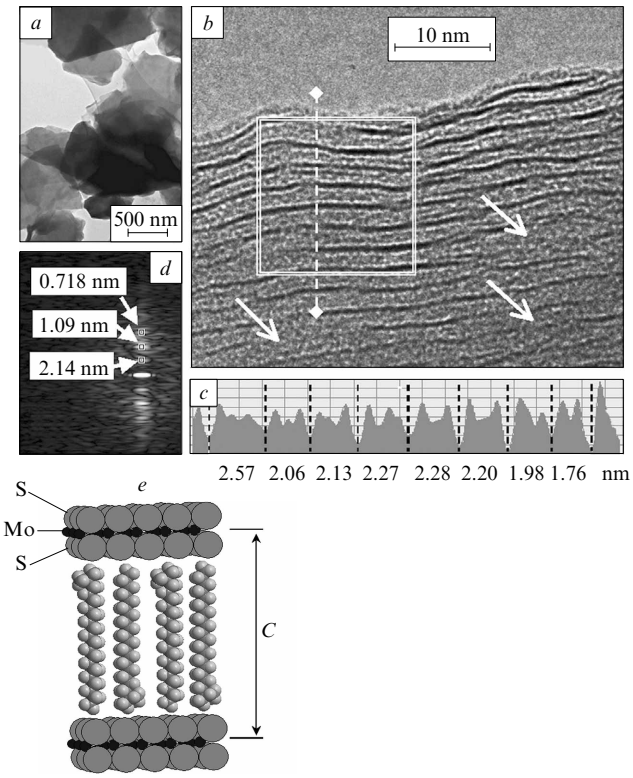


Figure 10. TEM image of the $[C_{18}H_{37}(CH_3)_3N]_{0.35}MoS_2$ particles (*a*); HRTEM image of the lateral projection of the structure; the arrows point to structure defects (*b*); TEM signal intensity profile along the line crossing the layers (*c*); FFT of the highlighted area (*d*) and the model of location of alkylammonium molecules between the MoS_2 layers (*e*).[48]

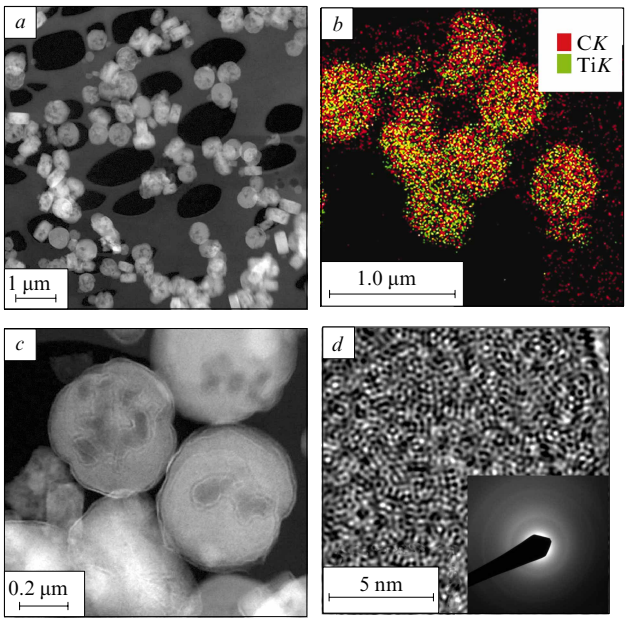


Figure 11. Images of the Ti – MIL-125 sample after 2,3,6-trimethylphenol oxidation to 2,3,5-trimethyl-1,4-benzoquinone. The micrographs were made by V.I.Zaikovskii (BIC SB RAS) by a procedure reported in Ref. 49.
(*a*) HAADF-STEM image, (*b*) Ti – C element map (HAADF-STEM – EDX), (*c*) mesoporous structure of globules, (*d*) HRTEM image after FFT filtration and electron diffraction pattern for the anatase-like structure.

had an unusual morphology: the disordered mesoporous amorphous particles ~500 nm in diameter consisted of small (~1 nm) dense corpuscles joined into globules and surrounded by concentric titanium-containing ~5 nm thick shells (see Fig. 11 *b*,*c*). After the third cycle, the shells disappeared and, according to HRTEM and SAED data, a weakly ordered anatase-like globular structure appeared (see Fig. 11 *d*, interlayer spacings: 0.35, 0.24, 0.19 nm, *etc*.).

III. Electron microscopy in the studies of organic molecular and hybrid systems

III.1. Methodological features of conducting a microscopy experiment

Organic compounds and reactions are studied much more rarely by electron microscopy than by the traditional methods such as nuclear magnetic resonance spectroscopy, infrared spectroscopy and mass spectrometry. The key factors that restrict the use of electron microscopy by organic chemists are as follows:

— traditional fine organic synthesis rarely involes samples investigation of which at micro- and nano-levels gives an amount of useful structure information comparable with the array of data on the molecular structure; the use of electron microscopy is justified only in relation to structured organic materials, polymers and so on;

— rather drastic conditions of observation; high vacuum in the sample chamber of the microscope precludes investigation of samples containing volatile components; neither highly volatile compounds as such nor virtually any solutions can be studied in this way; this actually precludes investigations of reactions *in situ*;

— high-energy electrons acting on organic samples can induce decomposition of compounds and, hence, structural information is lost.

The use of electron microscopy is restricted in the case of organic compounds without a complex structural organization and homogeneous organic reactions. Heterogeneous and colloid systems are more valuable objects for electron microscopy, but the drastic conditions of examination are still to be taken into account while planning the experiment in each particular case. In this respect, of interest is the publication,[50] which presents a quantitative estimate of the impact of electron beam on compounds containing light elements. The atom ejection cross-sections for model compounds (containing H, C and S) as functions of kinetic energy of the beam electrons are shown in Fig. 12. For relatively heavy elements such as carbon and sulfur, the curves have no maxima, the probability of atom ejection increasing monotonically with increasing electron energy. In the case of hydrogen, the curve has a clear-cut maximum at rather low electron beam energy, while after the maximum, the curve declines asymptotically.

Thus, the potential possibility of investigating organic compounds under drastic conditions inherent in the electron microscope can be expressed quantitatively. The energy 'windows' corresponding to low probability of atom ejection can be calculated and used in experiments.

Three approaches to investigating heterogeneous (or microheterogeneous) organic reactions by electron microscopy can be distinguished. The first one implies investigation of solid reactants or catalysts before the reaction, the second one consists in the study of the solid phase of the reaction mixture after it has been separated from other components, and the third one is to observe the behaviour of heterogeneous mixtures without pretreatment.

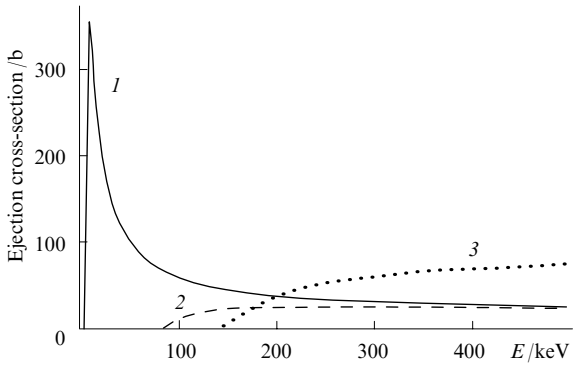


Figure 12. Ejection cross-sections of hydrogen (*1*), carbon (*2*) and sulfur (*3*) atoms as functions of the electron beam kinetic energy (E).[50]
Calculation for model compounds containing hydrogen, carbon and sulfur atoms.

In the first two cases, solid compounds, either neat or deposited on substrates, *e.g*., on aluminium foil, serve as the samples. Examination of these objects is preceded by the standard sample preparation procedure including the following operations: application of a minor amount of the sample on a special stage, attachment of the sample by means of a conductive adhesive or conductive adhesive tape, thorough drying of the sample and sputtering of a nanometre-thick metal or carbon layer onto the sample surface to provide the electrical conductivity and thus to suppress the charging effect, which impairs the image quality. However, it is noteworthy that metal sputtering should be used with caution, because it affects the sample morphology and chemical composition. For example, it was demonstrated[51] that sputtering of relatively thick (25 and 50 nm) chromium layers and 5 – 50 nm-thick layers of a palladium and platinum alloy results in deposition of well-discernable metal nanoparticles of about 5 – 15 nm size on the sample surface. This fact needs to be taken into account in the development of the sample preparation strategy and interpretation of the results of a microscopy examination. An adverse effect of the sputtering on the sample morphology can be avoided by using ultrathin coatings, by adjustment of the composition of the metal coating or by replacing metals or alloys by more neutral carbon.

For examination of heterogeneous systems without pretreatment, it is necessary to stabilize the liquid phase in vacuum. This problem can be solved by using special vacuum-tight capsules, which have a thin window transparent for the electron beam but simultaneously isolating the sample from the microscope chamber. Another approach implies the use of non-volatile ionic liquids either as the liquid phase of the sample or as a stabilizing matrix.

III.2. Application of electron microscopy for solution of particular research problems

Electron-microscopy study of the solid component of a reaction mixture before the reaction with subsequent determination of the activity or reactivity of this material is a common practice. Study of the activity of potassium permanganate acting as an oxidant in the oxidative coupling of

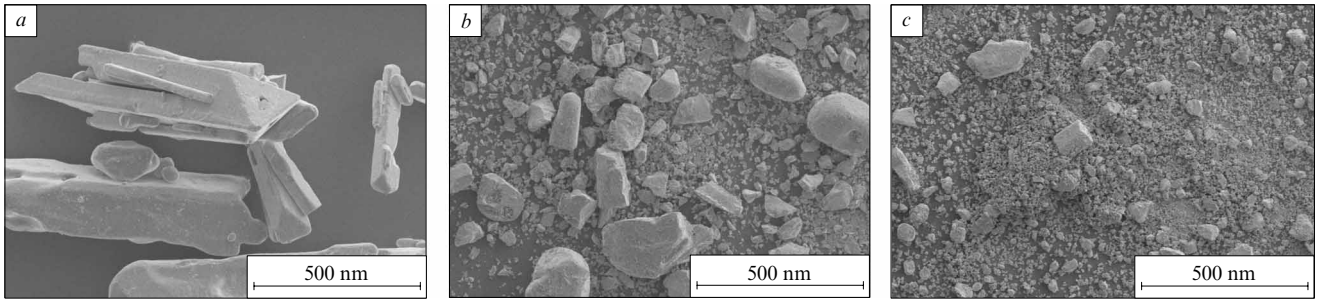


Figure 13. SEM images of $KMnO_4$ samples in the macrocrystalline form (*a*) and as coarse (*b*) and fine powder (*c*).[52]

oximes with 1,3-dicarbonyl compounds as a function of the degree of its dispersion can serve as an example.[52] It was shown that the use of the oxidant as a macrocrystalline compound or as a coarse powder may result in a 90% yield of the product of model reaction, while the use of fine powder under the same conditions gives a yield of 64%. The degree of dispersion was qualitatively evaluated on the basis of scanning electron-microscopy data (Fig. 13).

An increase in the activity of the cerium chloride catalyst in the addition of β-diketones to vinyl ketones on going from the macrocrystalline to microstructured state has been demonstrated.[53] When the initial macrocrystalline compound is used as the catalyst, the product yield in the model reaction is only 3%, whereas the use of microstructured $CeCl_3$ results in increasing the yield to 91%. The morphology of the catalyst was studied by scanning electron microscopy (Fig. 14).

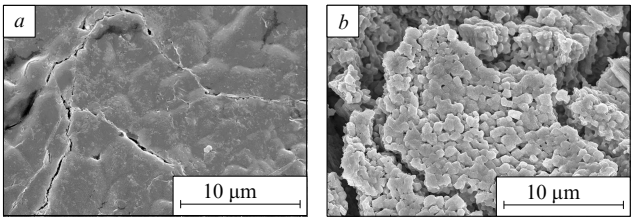


Figure 14. SEM images of $CeCl_3$ samples in the macrocrystalline (*a*) and microstructured forms (*b*).[53]

A similar activity increase of a heterogeneous catalyst upon dehydration, which is accompanied by appearance of a clear-cut microstructure, has been demonstrated[54] for peroxidation of β,δ-triketones in the presence of phosphomolybdic acid.

Scanning electron microscopy in combination with scanning transmission electron microscopy has proved useful in the studies of supported catalysts, which are also used in organic synthesis and in some other fields of catalytic chemistry. The morphology of palladium- and gold-based catalysts has been studied by STEM. The characterized catalysts have been successfully used in cross-coupling reactions,[55] liquid-phase hydrogenation,[56–58] oxidation of alcohols [59–61] and carbon monoxide oxidation.[62–63]

Hydrogenation of 1-phenylethynylphosphonic acid was used as an example to investigate the effect of the support on the palladium catalyst activity.[58] The authors demonstrated that the use of a material based on multiwalled carbon nanotubes and titanium dioxide ($MWCNT/TiO_2$) as the support gives a catalyst possessing high activity and stability. When 1 mol.% palladium was used, the yield of the hydrogenation product was 100% over more than 10 cycles of catalyst operation. The microstructures of $Pd/MWCNT/TiO_2$ and Pd/MWCNT were characterized by the BF-STEM technique (Fig. 15).

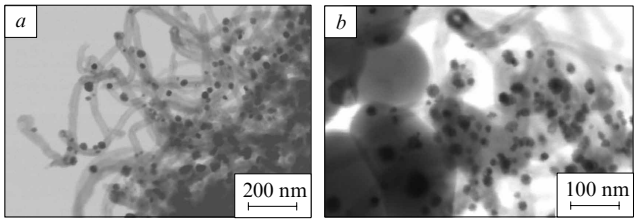


Figure 15. BF-STEM images of Pd/MWCNT (*a*) and $Pd/MWCNT/TiO_2$ (*b*). [58]

The same method was also successfully used to characterize the palladium nanoparticles in catalysts based on MOF — the metal-organic framework MIL-53(Al) and its modified analogue, (NH_2)–MIL-53(Al).[57] It was shown that palladium exists in the catalysts as nanoparticles of average size of not more than 4 nm (Fig. 16). The obtained Pd/MIL samples were tested in diphenylacetylene hydrogenation. The use of these catalysts was found afford *cis*-stilbene with a selectivity of more than 97% – 98% at a 95% conversion of the initial alkyne. It can be seen from the given examples that BF-STEM is a convenient tool for determining the shape and size of metal nanoparticles on solid substrates.

The SEM technique can serve to study the morphology of the support, because it has a higher sensitivity to surface

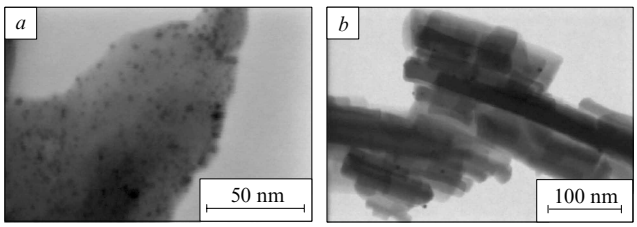


Figure 16. BF-STEM images of Pd/MIL-53(Al) (*a*) and $Pd/(NH_2)$–MIL-53(Al) (*b*).[57]

structure details than STEM (or TEM). Catalysts for selective reduction of nitrogen oxides have been studied by SEM.[64–66] The photomicrographs of the HBeta zeolite, used as one of the supports, and the (MnO_x-CeO_x)/HBeta catalyst (16% Mn–16% Ce) are shown in Fig. 17. According to electron-microscopy data, the catalyst surface structure with the supported MnO_x-CeO_x phase differed noticeably from the surface structure of the initial zeolite; this was attributed to the formation of a dense surface layer of the MnO_x-CeO_x particles.

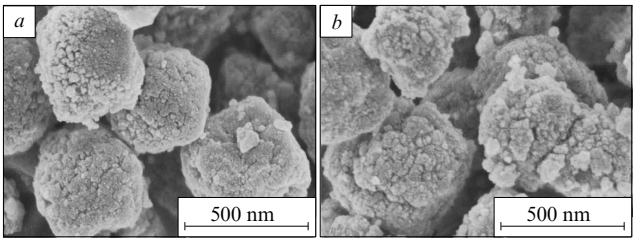


Figure 17. SEM images of HBeta (*a*) and (16% Mn–16% Ce)/HBeta (*b*).[66]

The possibility of applying electron microscopy to investigation of the microstructure of supported catalysts for fine organic synthesis processes was demonstrated in a study devoted to the use of the heterogeneous $Cu(ClO_4)_2/SiO_2$ catalyst in the peroxidation of β-diketones and β-ketoesters by *tert*-butyl hydroperoxide.[67] The SEM method was employed to examine the surface morphology of the catalyst obtained by deposition of $Cu(ClO_4)_2$ on SiO_2 from a solution in methanol and of the initial support (Fig. 18).

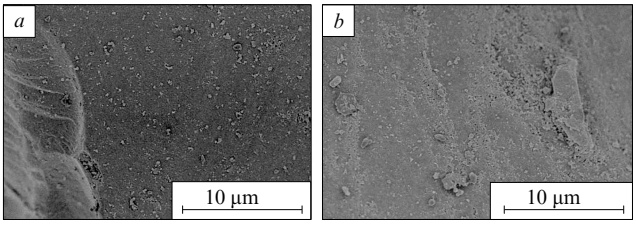


Figure 18. SEM images of SiO_2 (*a*) and $Cu(ClO_4)_2/SiO_2$ (*b*).[67]

The catalyst surface was found to resemble the surface of pure SiO_2. The catalyst exhibited a high activity towards peroxidation, the yield of peroxides was 65%–82%; the possibility of repeated use of the catalyst with a minor loss of activity was demonstrated.

In some cases, metal particles can be identified on the support surface by means of SEM. Usually, this is facilitated by a relatively large size and a distinguishable shape of metal particles and the nature of the support that gives an acceptable contrast level between the observed phases.

Studies devoted to the manufacture and use of cobalt-based catalysts for the Fischer–Tropsch synthesis can serve as an example of successful application of SEM for characterization of the catalyst active phase.[68, 69] For example, using electron microscopy, it was ascertained[69] that the active phase in the Co/Al_2O_3 and Co/SiO_2 supported

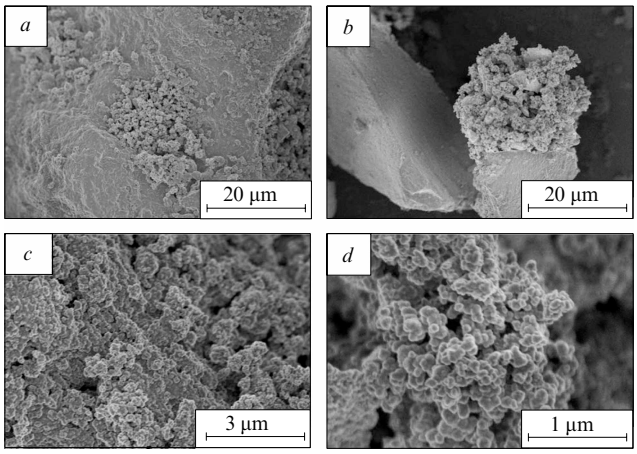


Figure 19. SEM images of Co/Al_2O_3 (*a*, *b*) and Co/SiO_2 (*c*, *d*).[69]

catalysts is represented by aggregated cobalt particles of 50–100 nm size (Fig. 19).

A contrast sufficient for visualization of even small metal particles can be attained for carbon-supported samples. This feature of the metal–support pair was used for detecting platinum particles in the active layer of a fuel cell electrode.[70] Metal particles of several nanometre size were detected as bright light dots on the carbon support surface (Fig. 20).

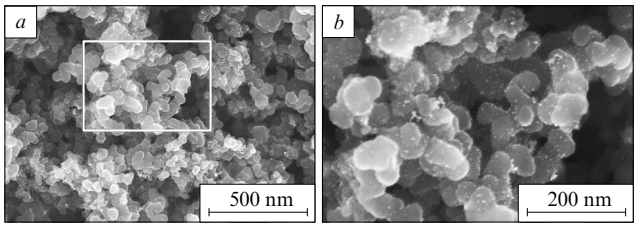


Figure 20. SEM images of platinum particles in the electrode active layer.[70]
(*a*) Survey micrograph, (*b*) enlarged fragment.

The ability of nano-sized metal particles to act as contrast agents in the metal–carbon system is used for defect visualization on a carbon support by the SEM method.[71] For this purpose, palladium particles are deposited on a carbon material from a solution of $Pd_2(dba)_3$ (dba is dibenzylideneacetone) in chloroform and then detected by electron microscopy (Fig. 21).

Analysis of particle distribution over the surface of a carbon material gives the idea of the presence of particular defects. The developed procedure was utilized to characterize various types of defects: point, linear, topological and so on. This procedure for defect visualization has been successfully used[72] to demonstrate the phenomenon of shielding of surface active sites on graphene by thin carbon films of 1–2 nm thickness.

It is noteworthy that dealing with free metal particles or uniform metallic films presents no difficulty. These objects are readily detected and their morphology can be studied with a relatively high resolution. Samples of such particles have high stability on exposure to electron beam. For

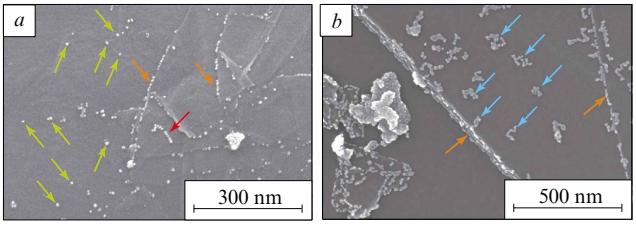


Figure 21. SEM images demonstrating the distribution of palladium particles on the surface of a carbon material.[71]
The arrows mark various types of defects: point, linear (*a*) and defects at graphene sheet boundaries (*b*).

example, palladium [73] and gold particles [74] and films based on them [75] have been investigated by electron microscopy. The photomicrographs of samples of palladium nanoparticles obtained upon decomposition of a chloroform solution of $Pd_2(dba)_3$ are presented in Fig. 22. The Pd particle size varies over a broad range from 60 to 200 nm. Smaller particles (10 – 20 nm) were detected in a minor quantity.

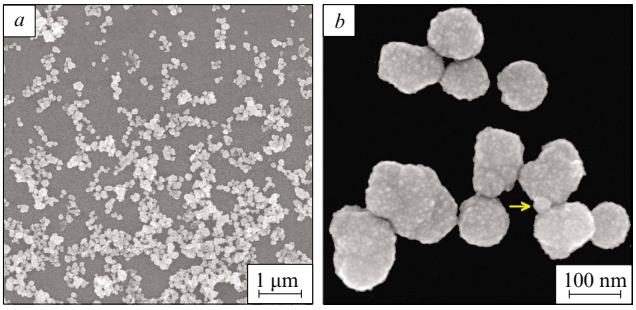


Figure 22. SEM images of palladium particles obtained upon decomposition of a solution of $Pd_2(dba)_3$ in chloroform.[73]
(*a*) Survey micrograph, (*b*) micrograph with high magnification; the arrow points to a small particle.

Most of the above examples were concerned with the use of micro- and nano-sized materials as catalysts of various chemical processes. However, reactions involving solid micro- or nanostructured reactants are equally important. Heterogeneous systems with solid-phase reactants are of interest because of the possibility to control the chemical properties of substances in such systems by controlling the morphology.

The photomicrographs of nanostructured coordination polymers with the formula $[Ni(SAr)_2]_n$ (Ar is aryl) are presented in Fig. 23. These compounds were shown [76] to undergo carbon – sulfur cross-coupling reactions with various aryl halides in the presence of copper or palladium compounds and triphenylphosphine to give the corresponding diaryl sulfides in up to 86% yields. It was also found that the reactivity of $[Ni(SAr)_2]_n$ particles is largely determined by their morphology. The high degree of structural organization of the coordination polymer accounts for its high activity in the cross-coupling.

In the general case, electron-microscopy investigation of the products of fine organic synthesis does not provide useful structural information; however, it is still used for investigations of self-assembled or other structured organic materials. As noted above, a substantial limitation is the

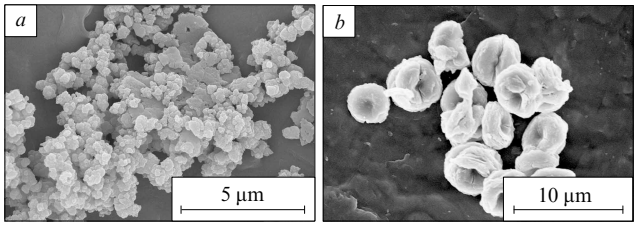


Figure 23. SEM photomicrographs of nanostructured samples of nickel aryl sulfides $[Ni(SAr)_2]_n$.[76]
Ar = Ph (*a*), 4-Br-C_6H_4 (*b*).

low stability of organic compounds to the action of electron beam. This problem can be solved quite easily by using low-voltage microscopy (in particular, with deceleration of electrons) and reduced currents of the electron beam. An additional advantage of these modes is a decrease in the contribution of the charging effects, which allows using materials without a special sample preparation.

The micrographs of the films of dimeric magnesium phthalocyanine complexes on aluminium foil are presented in Fig. 24. It was found [77] that upon self-assembly, phthalocyanine complexes form aggregates of different shape, most of them being spherical. The aggregate size varies from several hundred nanometres to several micrometres.

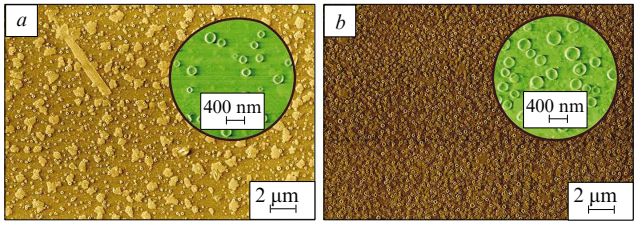


Figure 24. SEM images of films of dimeric magnesium phthalocyanine complexes. [77]
Figs *a* and *b* show the micrographs of two different complexes.

Using scanning electron microscopy, the structure of a micronized steroidal drug (mecigestone) substance was successfully studied.[78] The micrograph of the substance sputtered on the aluminium foil surface is shown in Fig. 25. The crystal size of the micronized drug is ~10 μm. According to biological testing, the bioavailability

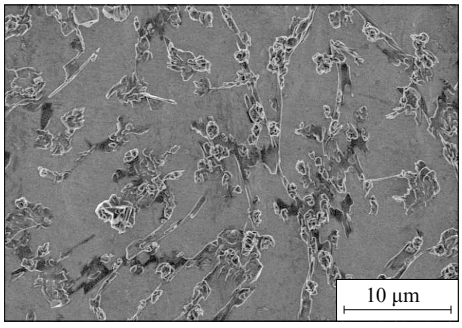


Figure 25. SEM image of the mecigestone drug substance.[78]

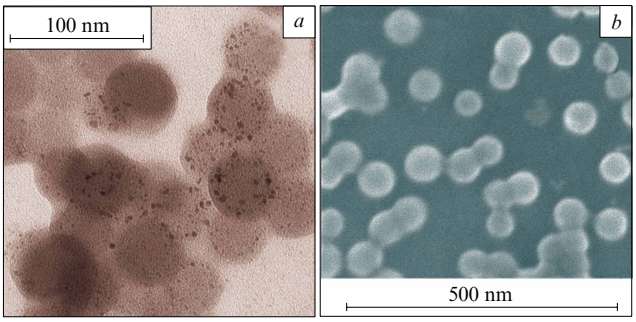


Figure 26. TEM (*a*) and SEM images (*b*) of the polystyrene and poly(4-vinylpyridine) block copolymer micelles decorated with palladium nanoparticles.[79]

of this agent was 7.5 times as high as that of the initial substance.

The structures of the polystyrene and poly(4-vinylpyridine) block copolymer micelles, both in the initial state and decorated with palladium nanoparticles, were characterized by a combination of atomic force, transmission and scanning electron microscopy.[79] The TEM and SEM images of micelles decorated with palladium nanoparticles are shown in Fig. 26. From transmission electron microscopy data, the metal particle size was determined to be $\sim$3 nm. Scanning electron microscopy served as an additional source of information about the morphology of the micelles acting as the support.

Using the low-voltage microscopy technique, it is possible to study not only organic compounds but also various materials of biological origin. Using scanning field emission electron microscopy, samples of bovine pericardium, which serves for the fabrication of prosthetic heart valves, were investigated.[80] The change in the surface morphology on treatment of pericardium samples with pure carbonic acid (Fig. 27) and a chitosan solution in carbonic acid was examined. On the basis of scanning electron microscopy data, the thickness of the deposited chitosan layer was investigated.

More examples of using electron microscopy to explore the structure of solid samples can be found in publications devoted to the microstructures of a number of metal-organic frameworks,[81–83] thermally expanded graphite,[84] iron oxide nanoparticles,[85] Ag – sapphire system[86] and silicon-containing film – laminated cloth systems.[87] Practically valuable results were obtained in a SEM study of

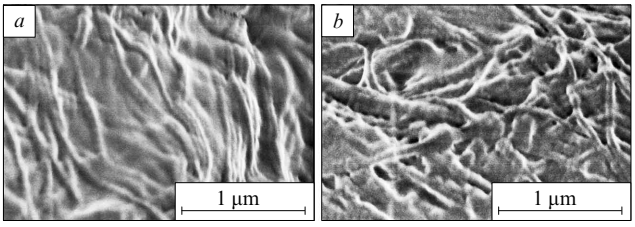


Figure 27. SEM images of bovine pericardium surface samples.[80] (*a*) In the initial form (stabilized with glutaraldehyde), (*b*) after carbonic acid treatment.

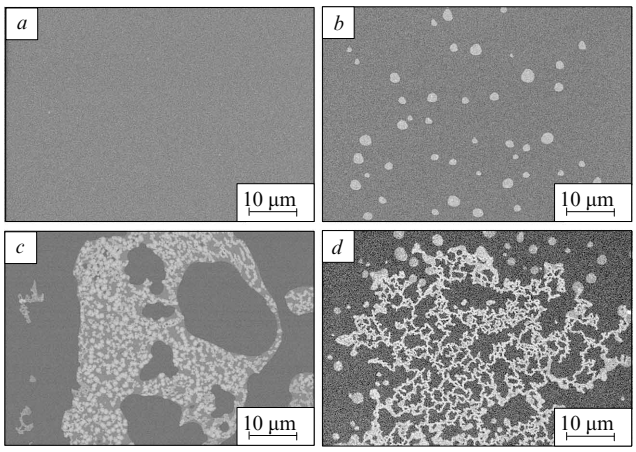


Figure 28. SEM images of [BMIM][BF_4] ionic liquid: in the pure state (*a*), with water traces (*b*) and with addition of 10 vol.% (*c*) and 20 vol.% of water (*d*).[89]

arabinogalactan inhibition of the deposition of calcium carbonate.[88]

The most interesting problem, from the standpoint of an organic chemist, that can be solved by electron microscopy is investigation of reaction mixtures 'as is' without isolation of the solid phase. This is a non-trivial task because the vast majority of solvents used in organic reactions cannot withstand high vacuum conditions in the sample chamber of an electron microscope. The only eligible type of solvents are ionic liquids. They have extremely low vapour pressure and remain stable in the chamber throughout the examination time.

Not only pure ionic liquids but also their mixtures with volatile compounds can be studied by SEM.[89] Figure 28 shows the micrographs of [BMIM][BF_4] ionic liquid in the pure state, with water traces and as a mixture with 10 vol.% and 20 vol.% of water added before the examination.

By means of electron microscopy, various structures formed by water in a solution in ionic liquid, such as droplets, dense structures and channels, were detected and described. In total, more than ten samples of binary mixtures of ionic liquids with water and alcohols were studied.[89]

Apart from binary systems, electron microscopy is suitable for investigation of reaction mixtures.[89] The micrographs of the reaction mixtures for conversion of fructose to 5-hydroxymethylfurfural in a [BMIM][BF_4] – [BMIM][Cl] mixture of ionic liquids in the presence of a catalyst (sulfuric

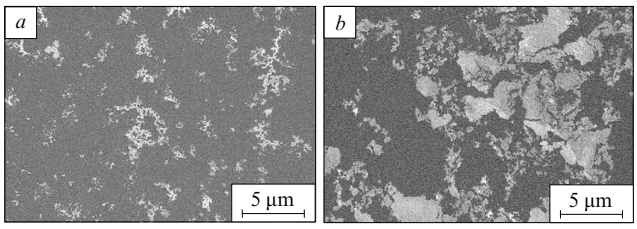


Figure 29. SEM images of samples of mixtures of fructose, sulfuric acid and ionic liquids containing traces (*a*) and 10 mass % of water (*b*).[89]

acid) and different amounts of water are presented in Fig. 29. The addition of 10 mass % of water to the reaction mixture promotes the formation of dense fructose aggregates, which has an adverse effect on the degree of conversion (20% *vs.* 66% for the system with water traces) to 5-hydroxymethylfurfural. Further research of the influence of water and conditions of synthesis resulted in the development of a special approach to the use of plant biomass in fine organic synthesis.[90]

IV. Conclusion

To summarize the presented material regarding the investigations of heterogeneous catalysts, we can distinguish two modern trends in the development of electron microscopy that are expected to prevail in the coming years:

— increase in the maximal resolution of electron-microscopic images to approach the atomic precision;

— necessary chemical analysis for assignment of contrasting elements of the image to particular catalyst components.

The former trend is related to the fact that in recent years, the sizes of the supported metal particles have been decreasing down to several nanometres. Simultaneously, the degree of dispersion of the metal has increased and, hence, the number of surface atoms on which the catalytic reaction takes place grows and the reactivity of these atoms changes; this brings about size effects. These effects can be used for practical purposes, especially for increasing the selectivity to the desired products in the selective oxidation and hydrogenation of hydrocarbons.[91 – 94] A clear demonstration of the trend towards decreasing the size of supported metal particles is switching to single atoms, which has become a rather popular line of research in recent years and has been called 'single atom catalysis'.[95, 96] Study of sintering processes of atoms and nanoparticles of supported metals, especially at the initial stage, is also exceptionally important for solving the problem of stability of supported heterogeneous catalysts.

The necessity of chemical analysis in microscopic experiments is dictated by vigorous development of bimetallic catalysts, because they often substantially enhance the catalytic processes compared with the processes catalyzed by monometallic samples.[97 – 100] It is clear that identification of particular elements of these catalysts is very important, as this makes it possible to determine the structure and spatial arrangement of elements, which is specified during the preparation of catalysts, and possible appearance of non-uniformity in bimetallic systems, for example, formation of monometallic particles. It is also noteworthy that the contrasts of some components of complex modified catalysts (*e.g.*, $Pd/CeO_2 - Al_2O_3$ catalysts for after-burning of exhaust gases) are very similar (PdO and CeO_2), which hampers identification of these components directly in the electron microscopy images.

Finally, TEM investigations during a catalytic reaction are also very important, because active sites of a different structure can be formed, and this would affect the catalytic reaction mechanism.[101]

While summarizing the presented material concerning organic synthesis, we would like to emphasize that modern chemical research is arriving to the level of preparation of complex molecules with high selectivity, which can conceptually be regarded as 'atomic precision'.[3, 4] It is the use of new-generation catalysts and advanced metal-containing materials that predetermined the rapid progress in the fine organic synthesis of molecular and hybrid systems with increasing complexity (Fig. 30). Electron microscopy has a primary role in characterization of micro- and nano-sized structural elements, and recent advances in the equipment have brought routine investigations to the atomic level.

Thus, for the first time, at the disposal of chemists, there is a versatile tool for visual detection of the morphological changes during the evolution of molecular and hybrid chemical systems (see Fig. 30). Apart from obtaining static images, electron microscopy was successfully used for video monitoring of physicochemical transformations in the liquid phase.[89] Within the framework of the ongoing project devoted to investigations of molecular and hybrid systems, the issues that are still unsolved in the methodology of organic chemistry and catalysis include visualization of processes with small molecules,[103 – 106] dynamic nature of complex biomolecules [107 – 110] and rational design of multifunctional systems.[111 – 114]

Obviously, the number of research works in classical organic chemistry performed with the aid of electron microscopy will markedly grow in the years to come. In the near future, electron microscopy is going to become an indis-

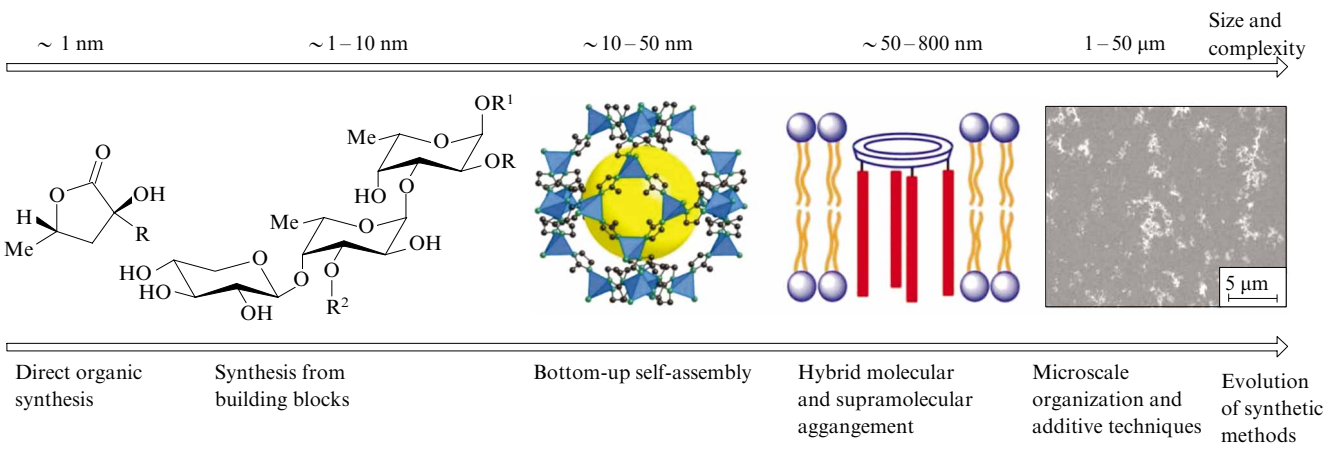


Figure 30. Formation of complex structures in the chemistry of molecular and hybrid systems.[102]

pensable and convenient tool for investigation of organic systems, like mass spectrometry and nuclear magnetic resonance.

This review was written with the financial support of the Russian Science Foundation (Project 14-23-00146 for the employees of BIC SB RAS and Project 14-50-00126 for employees of ZIOC RAS).

References

1. M P Egorov *Russ. Chem. Rev.* **83** (10) (2014)
2. I P Beletskaya, V P Ananikov *Rus. J. Org. Chem.* **51** 145 (2015) [*Zh. Org. Khim.* **51** 159 (2015)]
3. V P Ananikov, L L Khemchyan, Y V Ivanova, V I Bukhtiyarov, A M Sorokin, I P Prosvirin, S Z Vatsadze, A V Medved'ko, V N Nuriev, A D Dilman, V V Levin, I V Koptyug, K V Kovtunov, V V Zhivonitko, V A Likholobov, A V Romanenko, P A Simonov, V G Nenajdenko, O I Shmatova, V M Muzalevskiy, M S Nechaev, A F Asachenko, O S Morozov, P B Dzhevakov, S N Osipov, D V Vorobyeva, M A Topchiy, M A Zotova, S A Ponomarenko, O V Borshchev, Y N Luponosov, A A Rempel, A A Valeeva, A Y Stakheev, O V Turova, I S Mashkovsky, S V Sysolyatin, V V Malykhin, G A Bukhtiyarova, A O Terent'ev, I B Krylov *Russ. Chem. Rev.* **83** 885 (2014)
4. V P Ananikov, X Liu, U Schneider *Chem. Asian J.* **11** 328 (2016)
5. V V Kachala, L L Khemchyan, A S Kashin, N V Orlov, A A Grachev, S S Zalesskiy, V P Ananikov *Russ. Chem. Rev.* **82** 648 (2013)
6. A M Tsedilin, A N Fakhrutdinov, D B Eremin, S S Zalesskiy, A O Chizhov, N G Kolotyrkina, V P Ananikov *Mendeleev Commun.* **25** 454 (2015)
7. S S Zalesskiy, E Danieli, B Blumich, V P Ananikov *Chem. Rev.* **114** 5641 (2014)
8. T Kawasaki, T Yoshida, T Matsuda, N Osakabe, A Tonomura, I Matsui, K Kitazawa *Appl. Phys. Lett.* **76** 1342 (2000)
9. *What is the H3000 UHVEM?* Research Center for Ultra-High Voltage Electron Microscopy Osaka University. http://www.uhvem.osaka-u.ac.jp/en/what.html
10. S J Pennycook, M F Chisholm, A R Lupini, M Varela, A Y Borisevich, M P Oxley, W D Luo, K van Benthem, S-H Oh, D L Sales, S I Molina, Garcta-Barriocanal, C Leon, J Santamarta, S N Rashkeev, S T Pantelides *Philos. Trans. R. Soc. A* **367** 3709 (2009)
11. J Liu *J. Electron Microsc.* **54** 251 (2005)
12. *Energy-Filtering Transmission Electron Microscopy. Springer Series in Optical Sciences* Vol. 71 (Ed. L Reimer) (Berlin: Springer-Verlag, 1995)
13. *Progress in Transmission Electron Microscopy 1: Concepts and Techniques. Springer Series in Surface Sciences* Vol. 38 (Eds X-F Zhang, Z Zhang) (Berlin: Springer-Verlag, 2001)
14. S D Findlay, T Saito, N Shibata, Y Sato, J Matsuda, K Asano, E Akiba, T Hirayama, Y Ikuhara *Appl. Phys. Exp.* **3** 116603 (2010)
15. D Shindo, K Hiraga *High-Resolution Electron Microscopy for Materials Science* (Island Press, 1998)
16. R F Egerton *Electron Energy-Loss Spectroscopy in the Electron Microscope* (3rd Edn.) (New York: Springer Science Business Media, 2011)
17. M Weyland *Top. Catal.* **21** 175 (2002)
18. J Park, H Elmlund, P Ercius, J M Yuk, D T Limmer, Q Chen, K Kim, S H Han, D A Weitz, A Zettl, A P Alivisatos *Science* **349** 290 (2015)
19. B Goris, S Turner, S Bals, G Van Tendeloo *ACS Nano* **8** 10878 (2014)
20. V Klang, C Valenta, N B Matsko *Micron* **44** 45 (2013)
21. T Tsuda, N Nemoto, K Kawakami, E Mochizuki, S Kishida, T Tajiri, T Kushibiki, S Kuwabata *ChemBioChem* **12** 2547 (2011)
22. D S Su, B Zhang, R Schlögl *Chem. Rev.* **115** 2818 (2015)
23. W C H Kuo, M Briceno, D Ozkaya *Platin. Met. Rev.* **58** 106 (2014)
24. J M Thomas, C Ducati, R Leary, P A Midgley *ChemCatChem* **5** 2560 (2013)
25. G Van Tendeloo, S Bals, S Van Aert, J Verbeeck, D Van Dyck *Adv. Mater.* **24** 5655 (2012)
26. F M Ross *Science* **350** 9886 (2015)
27. M T Proetto, A M Rush, M-P Chien, P A Baeza, J P Patterson, M P Thompson, N H Olson, C E Moore, A L Rheingold, C Andolina, J Millstone, S B Howell, N D Browning, J E Evans, N C Gianneschi *J. Am. Chem. Soc.* **136** 1162 (2014)
28. Y Kimura, H Niinomi, K Tsukamoto, J M García-Ruiz *J. Am. Chem. Soc.* **136** 1762 (2014)
29. Y Liu, X-M Lin, Y Sun, T Rajh *J. Am. Chem. Soc.* **135** 3764 (2013)
30. F Tao, M Salmeron *Science* **331** 171 (2011)
31. S B Erenburg, S V Trubina, E A Kovalenko, O A Gerasko, V I Zaikovskii, D K Toporkov, K O Kvashnina, S G Nikitenko *J. Surf. Invest.* **9** 1031 (2015)
32. O A Gerasko, D G Samsonenko, V P Fedin *Russ. Chem. Rev.* **71** 741 (2002)
33. O V Belskaya, T I Gulyaeva, N N Leont,eva, V I Zaikovskii, T V Larina, T V Kireeva, V P Doronin,V A Likholobov *Kinet. Catal.* **52** 876 (2011) [*Kinet. Katal.* **52** 899 (2011)]
34. O Belskaya, L Stepanova, T Gulyaeva, S Erenburg, S Trubina, K Kvashnina, A Nizovskii, A Kalinkin, V Zaikovskii, V Bukhtiyarov, V Likholobov *J. Catal.* **341** 13 (2016)
35. O A Stonkus, L S Kibis, O Y Podyacheva, E M Slavinskaya, V I Zaikovskii, A H Hassan, S Hampel, A Leonhardt, Z R Ismagilov, A S Noskov, A I Boronin *ChemCatChem* **6** 2115 (2014)
36. E M Slavinskaya, R V Gulyaev, A V Zadesenets, O A Stonkus, V I Zaikovskii, Y V Shubin, S V Korenev, A I Boronin *Appl. Catal. B* **166** – **167** 91 (2016)
37. Z R Ismagilov, A E Shalagina, O Y Podyacheva, A V Ischenko, L S Kibis, A I Boronin, Y A Chesalov, D I Kochubey, A I Romanenko, O B Anikeeva, T I Buryakov, E N Tkachev *Carbon* **47** 1922 (2009)
38. O Y Podyacheva, Z R Ismagilov, A I Boronin, L S Kibis, E M Slavinskaya, A S Noskov, N V Shikina, V A Ushakov, A V Ischenko *Catal. Today* **186** 42 (2012)
39. S H Yang, W H Shin, J W Lee, H S Kim, J K Kang, Y K Kim *Appl. Phys. Lett.* **90** 013103 (2007)
40. O Scherzer *J. Appl. Phys.* **20** 20 (1949)
41. I E Beck, V I Bukhtiyarov, I Y Pakharukov, V I Zaikovsky, V V Kriventsov, V N Parmon *J. Catal.* **268** 60 (2009)
42. Z A Sabirova, M M Danilova, V I Zaikovskii, N A Kuzin, V A Kirillov, T A Kriger, V D Meshcheryakov, N A Rudina, O F Brizitskii, L N Khrobostov *Kinet. Catal.* **49** 428 (2008) [*Kinet. Katal.* **49** 449 (2008)]
43. M M Danilova, Z A Fedorova, V I Zaikovskii, A V Porsin, V A Kirillov, T A Krieger *Appl. Catal. B* **147** 858 (2014)
44. T M Yurieva, L M Plyasova, V I Zaikovskii, T P Minyukova, A Bliek, J C van den Heuvel, L P Davydova, I Y Molina, M P Demeshkina, A A Khassin, E D Batyrev *Phys. Chem. Chem. Phys.* **6** 4522 (2004)
45. T P Minyukova, N V Shtertser, A A Khassin, L M Plyasova, G N Kustova, V I Zaikovskii, Y G Shvedenkov, N A Baronskaya, J C van den Heuvel, A V Kuznetsova, L P Davydova, T M Yur'eva *Kinet. Catal.* **49** 821 (2008) [*Kinet. Katal.* **49** 685 (2008)]

46. A S Golub, V I Zaikovskii, N D Lenenko, M Danot, Y N Novikov *Russ. Chem. Bull., Int. Ed.* **53** 1914 (2004) [*Izv. Akad. Nauk, Ser. Khim.* 1837 (2004)]
47. A S Golub, N D Lenenko, V I Zaikovskii, Y N Novikov *Solid State Sci.* **14** 54 (2012)
48. N D Lenenko, E N Semina, V I Zaikovskii, A S Golub *Mater. Chem. Phys.* **141** 5 (2013)
49. O A Kholdeeva, I D Ivanchikova, N V Maksimchuk, M S Mel'gunov, J-S Chang, M Guidotti, A A Shutilov, V I Zaikovskii *Top. Catal.* **57** 1377 (2014)
50. T W Chamberlain, J Biskupek, S T Skowron, P A Bayliss, E Bichoutskaia, U Kaiser, A N Khlobystov *Small* **11** 622 (2015)
51. A S Kashin, V P Ananikov *Russ. Chem. Bull., Int. Ed.* **60** 2602 (2011) [*Izv. Akad. Nauk, Ser. Khim.* 2551 (2011)]
52. I B Krylov, A O Terent'ev, V P Timofeev, B N Shelimov, R A Novikov, V M Merkulova, G I Nikishin *Adv. Synth. Catal.* **356** 2266 (2014)
53. A O Terent'ev, V A Vil', I A Yaremenko, O V Bityukov, D O Levitsky, V V Chernyshev, G I Nikishin, F Fleury *New J. Chem.* **38** 1493 (2014)
54. A O Terent'ev, I A Yaremenko, A P Glinushkin, G I Nikishin *Russ. J. Org. Chem.* **51** 1681 (2015) [*Zh. Org. Khim.* **51** 1716 (2015)]
55. A N Kashin, O G Ganina, A V Cheprakov, I P Beletskaya *ChemCatChem* **7** 2113 (2015)
56. A Yu Stakheev, P V Markov, A S Taranenko, G O Bragina, G N Baeva, O P Tkachenko, I S Mashkovskii, A S Kashin *Kinet. Catal.* **56** 733 (2015) [*Kinet. Katal.* **56** 721 (2015)]
57. A Yu Stakheev, V I Isaeva, P V Markov, O V Turova, I S Mashkovskii, G I Kapustin, B R Saifutdinov, L M Kustov *Russ. Chem. Bull. Int. Ed.* **64** 284 (2015)
58. G N Bondarenko, O G Ganina, R K Sharma, I P Beletskaya *Russ. Chem., Bull., Int. Ed.* **63** 1856 (2014) [*Izv. Akad. Nauk, Ser. Khim.* 1856 (2014)]
59. E Redina, A Greish, R Novikov, A Strelkova, O Kirichenko, O Tkachenko, G Kapustin, I Sinev, L Kustov *Appl. Catal. A* **491** 170 (2015)
60. E A Redina, O A Kirichenko, A A Greish, A V Kucherov, O P Tkachenko, G I Kapustin, I V Mishin, L M Kustov *Catal. Today* **246** 216 (2015)
61. E A Redina, A A Greish, I V Mishin, G I Kapustin, O P Tkachenko, O A Kirichenko, L M Kustov *Catal. Today* **241** 246 (2015)
62. O A Kirichenko, N A Davshan, E A Redina, G I Kapustin, I V Mishin, O P Tkachenko, A V Kucherov, L M Kustov *Chem. Eng. J.* **292** 62 (2016)
63. O A Kirichenko, G I Kapustin, O P Tkachenko, V D Nissenbaum, I V Mishin, N A Davshan, E A Redina, L M Kustov *Mater. Res. Bull.* **80** 139 (2016)
64. A I Mytareva, D A Bokarev, G N Baeva, D S Krivoruchenko, A Yu Belyankin, A Yu Stakheev *Petrol. Chem.* **56** 211 (2016)
65. A Yu Stakheev, A I Mytareva, D A Bokarev, G N Baeva, D S Krivoruchenko, A L Kustov, M Grill, J R Thøgersen *Catal. Today* **258** 183 (2015)
66. D S Krivoruchenko, N S Telegina, D A Bokarev, A Yu Stakheev *Kinet. Catal.* **56** 741 (2015)
67. A O Terent'ev, V A Vil', O V Bityukov, G I Nikishin *Russ. Chem. Bull., Int. Ed.* **63** 2461 (2014) [*Izv. Akad. Nauk, Ser. Khim.* 2461 (2014)]
68. A P Savost'yanov, R E Yakovenko, S I Sulima, V G Bakun, G B Narochnyi, V M Chernyshev, S A Mitchenko *Catal. Today* (2016); doi: 10.1016/j.cattod.2016.02.037
69. O L Eliseev, M A Kamorin, P E Davydov, A S Volkov, A V Kazakov, A L Lapidus *Kinet. Catal.* **56** 625 (2015) [*Kinet. Katal.* **56** 634 (2015)]
70. I V Elmanovich, M S Kondratenko, D O Kolomytkin, M O Gallyamov, A R Khokhlov *Int. J. Hydr. Energy* **38** 10592 (2013)
71. E O Pentsak, A S Kashin, M V Polynski, K O Kvashnina, P Glatzel, V P Ananikov *Chem. Sci.* **6** 3302 (2015)
72. A E Sedykh, E G Gordeev, E O Pentsak, V P Ananikov *Phys. Chem. Chem. Phys.* **18** 4608 (2016)
73. S S Zalesskiy, V P Ananikov *Organometallics* **31** 2302 (2012)
74. S S Zalesskiy, A E Sedykh, A S Kashin, V P Ananikov *J. Am. Chem. Soc.* **135** 3550 (2013)
75. A P Simakova, M D Vedenyapina, V V Kuznetsov, N N Makhova, A A Vedenyapin *Russ. J. Phys. Chem. A* **88** 331 (2014)
76. A S Kashin, V P Ananikov *Top. Catal.* **56** 1246 (2013)
77. A Yu Tolbin, A V Dzuban, V I Shestov, Yu I Gudkova, V K Brel, L G Tomilova, N S Zefirov *RSC Adv.* **5** 8239 (2015)
78. A K Nazarov, I V Zavarzin, G V Nazarov, A V Aksenov, I S Levina *Pharm. Chem. J.* **49** 706 (2015) [*Khim.-Farm. Zh.* **49** (10) 44 (2015)]
79. M A Pigaleva, M V Bulat, G N Bondarenko, S S Abramchuk, T V Laptinskaya, M O Gallyamov, I P Beletskaya, M Moller *ACS Macro Lett.* **4** 661 (2015)
80. M O Gallyamov, I S Chaschin, M A Khokhlova, T E Grigorev, N P Bakuleva, I G Lyutova, J E Kondratenko, G A Badun, M G Chernysheva, A R Khokhlov *Mater. Sci. Eng. C* **37** 127 (2014)
81. V I Isaeva, A L Tarasov, V V Chernyshev, L M Kustov *Mendeleev Commun.* **25** 466 (2015)
82. V I Isaeva, M I Barkova, A V Kucherov, M M Ermilova, E V Orekhova, L M Kustov, A B Yaroslavtsev *Nanotechnol. Russ.* **9** 416 (2014)
83. E V Belyaeva, V I Isaeva, E E Said-Galiev, O P Tkachenko, S V Savilov, A V Egorov, L M Kozlova, V Z Sharf, L M Kustov *Russ. Chem. Bull., Int. Ed.* **63** 396 (2014) [*Izv. Akad. Nauk, Ser. Khim.* 396 (2014)]
84. D A Borisova, M D Vedenyapina, E D Strel'tsova, V L Maslov, K-H Rosenwinkel, D Weichgrebe, P Stopp, A A Vedenyapin *Solid Fuel Chem.* **47** 298 (2013)
85. A Stepanov, A Mustafina, R G Mendes, M H Rümmeli, T Gemming, E Popova, I Nizameev, M Kadirov *J. Iran. Chem. Soc.* **13** 299 (2016)
86. N A Toropov, P S Parfenov, T A Vartanyan *J. Phys. Chem. C* **118** 18010 (2014)
87. V V Andreev *Prikladnaya Fiz.* (6) 24 (2014)
88. F G Ishmuratov, E I Koptyaeva, A I Voloshin, A G Telin, Yu V Tomilov, N E Nifant'ev, V A Dokichev *Russ. J. Appl. Chem.* **88** 1920 (2015)
89. A S Kashin, K I Galkin, E A Khokhlova, V P Ananikov *Angew. Chem., Int. Ed.* **55** 2161 (2016)
90. K I Galkin, E A Khokhlova, L V Romashov, S S Zalesskiy, V V Kachala, J V Burykina, V P Ananikov *Angew. Chem., Int. Ed.* **55** 8338 (2016)
91. A M Gololobov, I E Bekk, G O Bragina, V I Zaikovskii, A B Ayupov, N S Telegina, V I Bukhtiyarov, A Yu Stakheev *Kinet. Catal.* **50** 830 (2009) [*Kinet. Katal.* **50** 864 (2009)]
92. B L Moroz, P A Pyrjaev, V I Zaikovskii, V I Bukhtiyarov *Catal. Today* **144** 2927305 (2009)
93. I L Simakova, Yu S Solkina, B L Moroz, O A Simakova, S I Reshetnikov, I P Prosvirin, V I Bukhtiyarov, V N Parmon, D Yu Murzin *Appl. Catal. A* **385** 136 (2010)
94. E A Artiukha, A L Nuzhdin, G A Bukhtiyarova, S Yu Zaytsev, P E Plyusnin, Yu V Shubin, V I Bukhtiyarov *Catal. Sci. Technol.* **5** 4741 (2015)
95. J D Kistler, N Chotigkrai, P H Xu, B Enderle, P Praserthdam, C-Y Chen, N D Browning, B C Gates *Angew. Chem., Int. Ed.* **53** 8904 (2014)
96. B Qiao, J-X Liang, A Wang, C-Q Xu, J Li, T Zhang, J J Liu *NanoRes.* **8** 2913 (2015)
97. V Ponec *Appl. Catal. A* **222** 31 (2001)

98. J C Pritchard, Q He, E N Ntainjua, M Piccinini, J K Edwards, A A Herzing, A F Carley, J A Moulijn, C J Kiely, G J Hutchings *Green Chem.* **12** 915 (2010)
99. F Gao and D W Goodman *Chem. Soc. Rev.* **41** 8009 (2012)
100. A Wang, X Y Liu, C-Y Mou, T Zhang *J. Catal.* **308** 258 (2013)
101. I Y Pakharukov, A Y Stakheev, I E Beck, Y V Zubavichus, V Yu Murzin, V N Parmon, V I Bukhtiyarov *ACS Catal.* **5** 2795 (2015)
102. V P Ananikov, K I Galkin, M P Egorov, A M Sakharov, S G Zlotin, E A Redina, V I Isaeva, L M Kustov, M L Gening, N E Nifantiev *Mendeleev Commun.* **26** 365 (2016)
103. S G Zlotin, S V Kochetkov *Russ. Chem. Rev.* **84** 1077 (2015)
104. V G Lisnyak, A S Kucherenko, E F Valeev, S G Zlotin *J. Org. Chem.* **80** 9570 (2015)
105. E V Filatova, O V Turova, I V Kuchurov, A A Kostenko, A G Nigmatov, S G Zlotin *J. Supercrit. Fluids* **109** 35 (2016)
106. S G Zlotin, A M Churakov, O A Luk'yanov, N N Makhova, A Yu Sukhorukov, V A Tartakovsky *Mendeleev Commun.* **25** 399 (2015)
107. B S Komarova, M V Orekhova, Y E Tsvetkov, R Beau, V Aimanianda, J-P Latge, N E Nifantiev *Chem. Eur. J.* **21** 1029 (2015)
108. B S Komarova, Y E Tsvetkov, N E Nifantiev *Chem. Rec.* **16** 488 (2016)
109. A Roy, T Saha, M L Gening, D V Titov, A G Gerbst, Y E Tsvetkov, N E Nifantiev, P Talukdar *Chem. Eur. J.* **21** 17445 (2015)
110. N E Ustyuzhanina, M I Bilan, A G Gerbst, N A Ushakova, E A Tsvetkova, A S Dmitrenok, A I Usov, N E Nifantiev *Carbohydr. Polym.* **136** 826 (2016)
111. M Zabilskiy, P Djinović, E Tchernychova, O P Tkachenko, L M Kustov, A Pintar *ACS Catal.* **5** 5357 (2015)
112. V I Isaeva, M I Barkova, L M Kustov, D A Syrtsova, E A Efimova, V V Teplyakov *J. Mater. Chem. A* **3** 7469 (2015)
113. O P Tkachenko, A A Greish, A V Kucherov, K C Weston, A M Tsybulevski, L M Kustov *Appl. Catal. B* **179** 521 (2015)
114. N Chilingarov, A Medvedev, G Deyko, L Kustov, E Chernikova, L Glukhov, V Markov, V Senyavin, M Polyakova, L Sidorov *Rapid Commun. Mass Spectrom.* **29** 1227 (2015)